MOLECULAR AND CELLULAR BIOLOGY, Feb. 1989, p. 541–550
0270-7306/89/020541-10$02.00/0

Vol. 9, No. 2

Mapping In Vivo Topoisomerase I Sites on Simian Virus 40 DNA: Asymmetric Distribution of Sites on Replicating Molecules

STEPHANIE E. PORTER AND JAMES J. CHAMPOUX*

Department of Microbiology, School of Medicine, University of Washington, Seattle, Washington 98195

Received 16 August 1988/Accepted 31 October 1988

Complexes between simian virus 40 DNA and topoisomerase I (topo I) were isolated from infected cells treated with camptothecin. The topo I break sites were precisely mapped by primer extension from defined oligonucleotides. Of the 56 sites, 40 conform to the in vitro consensus sequence previously determined for topo I. The remaining 16 sites have an unknown origin and were detectable even in the absence of camptothecin. Only 11% of the potential break sites were actually broken in vivo. In the regions mapped, the pattern of break sites was asymmetric. Most notable are the clustering of sites near the terminus for DNA replication and the confinement of sites to the strand that is the template for discontinuous DNA synthesis. These asymmetries could reflect the role of topo I in simian virus 40 DNA replication and suggest that topo I action is coordinated spatially with that of the replication complex.

Topoisomerases are enzymes that change the superhelical state of DNA by transiently breaking one or both strands of the duplex. Type II topoisomerases make a staggered double-strand break, whereas the type I enzymes introduce a single-strand break. The known eucaryotic topoisomerases are capable only of relaxing supercoiled DNA, whereas some of the bacterial enzymes are able to introduce supercoils (e.g., DNA gyrase in *Escherichia coli*) (for recent reviews, see references 39 and 62 to 64). The eucaryotic type I topoisomerase (topo I) attaches covalently to the 3′ end of the nicked strand, forming a DNA-protein intermediate in the nicking-closing reaction (11–13). This covalent intermediate can be trapped in vitro by stopping the enzyme reaction with sodium dodecyl sulfate (SDS) or alkali (10).

Topo I break sites were previously mapped in vitro by stopping the reactions with SDS or alkali and analyzing the breakage products on sequencing gels (3). Over 200 rat liver topo I sites were mapped on linear fragments of purified simian virus 40 (SV40) DNA. A compilation of the nucleotides surrounding the break sites revealed the following degenerate consensus sequence for topo I breakage: 5′-A/T-G/C-T/A-T-3′, with the 3′ nucleotide being the one to which topo I attaches. The formation of covalent protein-DNA complexes in vitro can be greatly increased by the addition of the cytotoxic alkaloid camptothecin (CTT) (27). Although CTT enhances the cleavage at some sites to a greater extent than at other sites, the basic pattern of topo I cleavage with and without the drug is nearly the same (32; J. J. Champoux and R. Aronoff, J. Biol. Chem., in press). It appears that CTT acts to slow or block the reclosure step of the nicking-closing reaction, thereby increasing the amount of enzyme trapped in the covalently bound state when the reaction is stopped with detergent (Champoux and Aronoff, in press).

In *E. coli*, the type I topoisomerase acts in opposition to DNA gyrase, preventing excessive negative supercoiling of the chromosomal DNA (19, 43). The function of the eucaryotic enzyme is, however, less well defined. In *Saccharomyces cerevisiae*, mutants deleted for topo I are still viable, although it is possible that the topoisomerase II (topo II) can compensate for the loss of type I activity (6, 58). The phenotype of yeast topo I-topo II double mutants suggests that topo I is involved in both DNA replication and transcription (6). Recent experiments also implicate the enzyme in SV40 DNA replication (see below). Support for a role in transcription comes from several lines of evidence in higher eucaryotes. Topo I has been found in abundance at the sites of actively transcribing genes in diverse systems such as the rRNA genes of *Tetrahymena* spp., *Xenopus* spp., and humans (4, 17, 71); the heat shock genes of *Drosophila* spp. (21, 22); and the tyrosine aminotransferase gene of rats (51). It may play a role in transcription by acting ahead of or behind the RNA polymerase to relieve the superhelical tension generated by movement of the transcribing complex along the helix (36, 68).

Recent evidence suggests that the eucaryotic topo I may also be involved in illegitimate recombination (15). Provided with a variety of special substrates in vitro, the enzyme can break the DNA and subsequently rejoin two strands from different molecules (16, 23, 40). Results of an analysis of sequences surrounding the break sites involved in illegitimate recombination are consistent with the involvement of topo I as a component in an illegitimate recombination pathway in vivo (8, 15).

SV40 is a double-stranded DNA virus that has been used extensively as a model for mammalian DNA replication. The viral DNA is replicated bidirectionally from a unique origin (ori), has a nucleosome structure that gives it the appearance of a minichromosome, and requires only one virally encoded protein (the T antigen) for its replication (see reference 59 for a review). Many of the details of SV40 replication have been defined. The start sites for the initiation of both continuous and discontinuous DNA synthesis in the vicinity of the origin are known (24, 61). The nucleosome structure of the SV40 minichromosome has been extensively studied (28, 41, 48, 52). Approximately 20% of the molecules have a nucleosome-free area that spans roughly 400 bases, including the origin, and that is unusually sensitive to restriction enzymes and nucleases (31, 42, 44, 49, 60). The terminus of DNA replication has been mapped and does not appear to display the same type of sequence specificity as found for the ori region. The majority of replicating SV40 molecules terminate approximately 180° from the ori (59, 65), although some

* Corresponding author.

molecules terminate replication at other more distant sites (54).

Topoisomerases are required for SV40 DNA replication both in vitro (70) and in vivo (2, 14, 46, 47), although the relationship between the type I and type II activities is unclear. It appears that topo I is insufficient for complete replication in cellular extracts, since in the absence of topo II a catenated dimer is the final product of replication. Thus, the type II enzyme is required in vitro for the segregation of replicated daughter molecules, while the type I topoisomerase does not seem to be essential. In vivo the situation is more complex, since inhibition of topo II does not result in the production of catenated dimers, as might be predicted from the in vitro results (69). Also, topo I is found associated preferentially with replicating SV40 molecules in vivo (14), suggesting that topo I plays a vital role in viral replication in the infected cell.

Since the sequence specificity of topo I was previously determined in vitro on naked DNA, it was of interest to establish the specificity of the enzyme on native chromatin in vivo. In this study, CTT was used to map a large number of in vivo topo I break sites on SV40 DNA. We have identified two types of break sites in the present analysis. The majority conform well to the in vitro consensus sequence and are termed consensus-type sites. The other sites seem to have no relation to the in vitro sequence and are termed nonconsensus-type sites. It is significant that topo I appears to be acting at only a small fraction of the potential consensus-type sites. Those sites that are broken exhibit an interesting asymmetrical distribution on the SV40 genome.

MATERIALS AND METHODS

Enzymes. Klenow fragment, T4 polynucleotide kinase, and the Sequenase kit were purchased from U.S. Biochemical Corp.; *Eco*RI was purchased from Bethesda Research Laboratories, Inc.; *Eco*NI and T4 DNA ligase were purchased from New England BioLabs, Inc.; pancreatic DNase I was purchased from Millipore Corp.; and proteinase K was purchased from Beckman Instruments, Inc.

Cell culture and virus infection. An African green monkey kidney cell line (CV-1) was grown on plastic dishes (diameter, 10 cm; Lux Scientific Corp.) in 10 ml of Dulbecco modified Eagle medium (DME) supplemented with 10% newborn calf serum (GIBCO Laboratories). Cells were grown to confluency and infected at a multiplicity of approximately 20 PFU per cell with a clone of SV40 VA45-54, obtained from P. Tegtmeyer (57). The cloned strain has a DNA sequence that differs slightly from the published sequence (7) as delineated by Been et al. (3). At 40 h postinfection, the growth medium was replaced with 2 ml of DME that contained CTT at a final concentration of 10 μM (CTT lactone [NSC 94600] was obtained from the Natural Products Division, National Cancer Institute, Bethesda, Md.). The CTT was stored as a 10 mM stock solution in dimethyl sulfoxide. The cells were treated with CTT for 5 min immediately prior to detergent lysis (see below). Some cells were mock treated by being subjected to the above procedure in the absence of CTT.

Extraction of viral DNA. The method of Hirt was used to extract the viral DNA (25). Briefly, the cells were lysed by the addition of 0.8 ml of a solution containing 50 mM Tris hydrochloride (pH 7.5), 10 mM EDTA, and 0.6% SDS. After incubation at 20°C for 10 min, 0.2 ml of 5 M NaCl was added to each plate. After gentle rocking to mix the lysate, it was poured into a 10-ml plastic centrifuge tube. The cellular DNA was removed by precipitation at 4°C overnight and centrifugation at 10,000 rpm for 30 min in a Beckman JA20 rotor.

Purification of DNA and DNA-protein complexes by neutral CsCl equilibrium centrifugation. The Hirt supernatant from the lysis of five plates of cells was diluted to 7.7 ml with 10 mM Tris hydrochloride (pH 7.5)–1 mM EDTA (TE), and 9.2 g of CsCl was added (final density, 1.67 g/ml). Where indicated, samples were pretreated with proteinase K (50 μg/ml) for 1 h at 37°C. ^{3}H-labeled SV40 DNA was added as a density marker, and the samples were centrifuged in a Beckman VTi65 rotor at 50,000 rpm for 16 h. Fractions (12 drops each, approximately 180 μl) were collected in 1.6-ml plastic centrifuge tubes, and 10 μl of each was spotted onto Whatman 3MM filter disks (diameter, 2.3 cm). The filters were washed in 5% trichloroacetic acid and then in 95% ethanol. After the filters were dried, the radioactivity was counted in a toluene-based scintillation fluid in a Beckman LS 3801 liquid scintillation counter. The first two or three fractions at the front of the high-density peak (^{3}H marker) were pooled as the high-density sample. The high-density peak contained a mixture of SV40 supercoiled and nicked circular DNAs. The fractions constituting the low-density sample were pooled starting at the second fraction after the ^{3}H marker DNA peak had declined to the background level and ending at the top of the gradient. This region of the gradient has been previously shown to contain the protein-bound DNA (14). The pooled fractions were treated with proteinase K (30 μg/ml) for 60 min at 37°C, and the samples were dialyzed against 1 liter of TE with three changes for 4 to 12 h each at 20°C. The samples were phenol and chloroform extracted. Bovine serum albumin was added as the carrier (2 μg/ml), and the DNA was precipitated with ethanol in the presence of 0.3 M sodium acetate. The low-density samples were dissolved in 12 μl of TE, and the high-density samples were dissolved in 20 μl of TE.

Preparation of sample for protein gel and Western blotting. The isolation of low- and high-density samples was identical to that described above through the stage of pooling the appropriate CsCl fractions. Carrier DNA was added to the low-density sample to approximately 20 μg/ml, and the samples were precipitated from CsCl directly by dilution with an equal volume of TE and addition of 2 volumes of room temperature ethanol. The precipitate was collected by centrifugation at 10,000 rpm for 30 min in a Beckman JA-20 rotor and dissolved in 2 ml of TE. The ethanol precipitation was repeated twice, and the samples were dissolved in TE. For samples that were to be treated with DNase I, $MgCl_2$ was added to 6 mM and DNase I was added to 100 μg/ml. The samples were incubated for 60 min at 37°C, and the reaction was stopped by addition of EDTA to 27 mM and NaOH to 0.2 N. All of the above steps took place in the same 15-ml Corex tube to avoid loss of sample. Insulin (50 μg/ml) was added as the carrier, and the samples were precipitated with trichloroacetic acid (final concentration, 10%), washed with acetone, and reprecipitated. The samples were dissolved in 15 μl of Laemmli loading buffer (33).

The samples were boiled for 5 min and loaded on a Laemmli gel (33) consisting of 10% polyacrylamide–*N*,*N*′-diallyltartardiamide (DATD), with a 3% polyacrylamide stacking gel. The running buffer contained 23 g of glycine, 4.8 g of Trizma base, and 1.6 g of SDS in a final volume of 1.6 liters. The samples, including molecular weight standards from BioRad Laboratories, were electrophoresed at 15 mA for 1.5 h in the Hoefer Mighty Small II protein gel electrophoresis system. The CV-1 whole-cell extract control was

prepared by scraping the cells from a confluent plate (approximately 10^7 cells) and suspending them in Tris-buffered saline (25 mM Tris hydrochloride [pH 7.4], 135 mM NaCl, 5 mM KCl, 0.7 mM Na_2HPO_4). Approximately 10^6 cells were pelleted, suspended in 15 μl of Laemmli loading buffer, and boiled for 5 min. After electrophoresis, the material in the gel was transferred to a nitrocellulose membrane by using the Hoefer TE22 Transphor system and a transfer buffer containing 6.1 g of Trizma base, 28.8 g of glycine, and 400 ml of methanol in a final volume of 2 liters. The filter was blocked in a milk-based solution of 10% nonfat dry milk in TTBS (TTBS is 0.05% Tween 20, 20 mM Tris hydrochloride [pH 7.5], plus 0.5 M NaCl), washed in TTBS, and reacted with human anti-human topo I (Scl-70 serum from Alpha Antigens, Inc.). After being washed again, the filter was reacted with the secondary antibody, goat anti-human immunoglobulin G conjugated to horseradish peroxidase (from BioRad), and developed as specified by the manufacturer.

Primer extensions and sequencing reactions. Oligonucleotide primers 18 nucleotides in length were synthesized on a Biosearch model 8600 DNA synthesizer. The oligonucleotides were purified through a 20% polyacrylamide–8 M urea gel. The bands were excised, eluted in TE, and adsorbed to a Sep-Pak C-18 column (Waters Associates, Inc.). The oligonucleotides were eluted with 60% methanol–4 mM triethylammonium carbonate, lyophilized, and stored frozen in distilled water. Oligonucleotide primers were labeled to approximately 2×10^6 cpm/pmol with [γ-^{32}P]ATP (3,000 Ci/mmol; Du Pont, NEN Research Products) and T4 polynucleotide kinase. For generating the dideoxy-sequencing ladders, the primers were used in conjunction with the Sequenase kit by following the protocol supplied by the manufacturer. The template for dideoxy-sequencing reactions was the single-stranded form of the plasmid pBSMSV2 or pBSMSV5 (identical except for the orientation of the insert). This plasmid was constructed by cloning SV40 into the *Eco*RI site of the vector pBSM13+ (Stratagene).

The primer extensions on the low- and high-density samples were performed by the following method. High-density (1 μl) or low-density (2.6 μl) sample was mixed with 1.7 ng of ^{32}P-end-labeled primer in the presence of 70 mM Tris hydrochloride (pH 7.5), 15 mM $MgSO_4$, 0.1 mM dithiothreitol, and 50 mg of bovine serum albumin per ml. The reaction mixtures were boiled for 3 min to denature the double-stranded DNA and chilled in an ice-water bath for 5 min. A mix of dATP, dTTP, dCTP, and dGTP was added such that each deoxynucleoside triphosphate was at a final concentration of 400 μM, and the reaction mixtures were brought up to 6.4 μl with H_2O. They were then warmed to 37°C for 2 min, 1 U of Klenow fragment was added, and the extensions were allowed to proceed for 20 min. The reactions were terminated by adding 4.4 μl of formamide-loading dye mix (Sequenase kit), and the mixtures were boiled for 3 min just before being loaded on a sequencing gel.

Sequencing gels. The samples were analyzed by electrophoresis in either 5% or 8% polyacrylamide gels containing 8 M urea (38). The samples (5 μl each) were loaded such that for each set of reactions a low-density peak sample appeared next to a minimum of three different sequencing reactions, typically the T, G, and C lanes (see Fig. 2A). The high-density material was used as a primer extension control; thus, bands appearing in both the high- and low-density lanes were not considered to be break sites. To be counted as a site, the relative intensity of the band in the low-density lane had to be at least twofold higher than a background band in the control lane. The samples were electrophoresed for 5 to 10 h at 1,000 to 1,800 V, depending on the percentage of acrylamide. Gels were dried under vacuum on a Hoefer model SE1150 dual-slab gel drier. The dried gels were exposed to Kodak XAR-2 film (35 by 43 cm) for 1 to 8 days.

RESULTS

Mapping in vivo topo I break sites by using CTT. The CV-1 line of African green monkey kidney cells was grown to confluency and infected with SV40. The cells were treated for 5 min with CTT 40 h postinfection, when the rate of SV40 DNA replication was near maximal (56). The viral DNA was extracted by the method of Hirt (25) and fractionated by CsCl equilibrium centrifugation. The viral DNA distributed in the gradient as two distinct populations: a low-density peak that contained SV40 DNA tightly associated with protein (see below), and a high-density peak that contained protein-free SV40 DNA (14). After fractionation, the samples were treated with proteinase K to remove any bound protein. The low-density material isolated after treatment with CTT contains replicating SV40 molecules that have been trapped as covalent complexes with topo I (14; see below). This low-density material represented 7 to 10% of the total SV40 DNA in the gradient (data not shown).

The topo I break sites were mapped by primer extension. The low- and high-density samples were denatured with heat and annealed to a specific ^{32}P-end-labeled oligonucleotide primer. The primer was extended with Klenow fragment, and the runoff products were analyzed by electrophoresis in either a 5% or 8% sequencing gel alongside dideoxy-sequencing ladders. The high-density peak, which did not show specific breaks due to topo I, served as a control for artifacts of the technique such as Klenow pausing or non-protein-associated breaks. Figure 1 illustrates the results of a typical experiment. The low-density (lane L) and high-density (lane H) primer extension products are shown alongside the dideoxy-sequencing lanes (lanes A, C, G, and T). The arrowheads point to five topo I break sites, identified by their unique appearance in lane L. The sequence surrounding one of these sites is expanded to the right of the gel (dotted arrow) as an example of the mapping technique. As is discussed below in more detail (see Fig. 4), the sites mapped in this way fall into two categories. The majority conform well to the consensus sequence previously found for topo I breakage in vitro (3). These are termed consensus-type sites. The other sites do not have any obvious relation to the in vitro sequence and are termed non-consensus-type sites.

The break sites in the low-density pool are associated with protein. To be certain that the sites being mapped were indeed associated with bound protein, we treated a portion of the Hirt-extracted DNA with proteinase K before CsCl equilibrium centrifugation. This treatment should cause SV40 molecules that had contained bound topo I to band at the position of high-density DNA, rather than at the usual low-density position. Pretreatment with proteinase K eliminated the topo I-related primer extension products from the low-density sample (Fig. 2A, compare lane 4 with lanes 1 and 2 at the position of the arrowheads). In fact, the original autoradiogram clearly showed that these bands had shifted into the high-density sample (Fig. 2A, compare bands at top arrowhead in lanes 2 and 5).

To confirm that the low-density material contained topo I bound to DNA, the sample preparation procedure was altered to isolate intact protein-DNA complexes for Western immunoblot analysis (see Materials and Methods). The

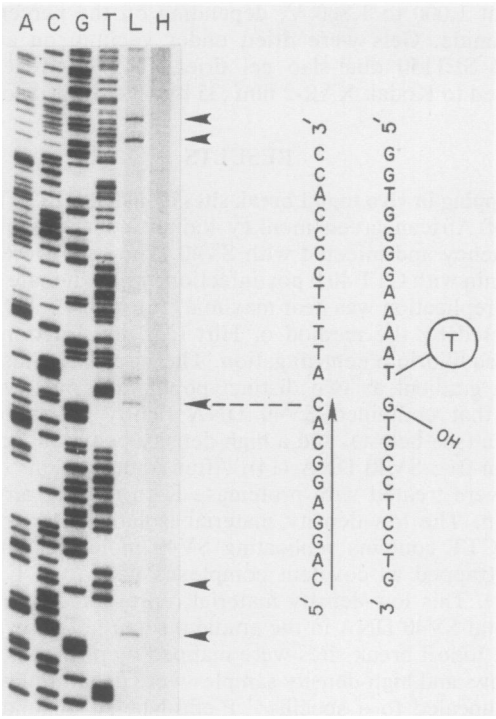

FIG. 1. Mapping of in vivo topo I break sites on SV40 DNA. SV40 DNA was isolated from infected CV-1 cells that had been treated with CTT. The DNA was fractionated on a CsCl gradient to yield a low-density (lane L), protein-associated pool and a high-density (lane H), non-protein-associated peak. The samples were denatured with heat and used as templates for primer extension with the ^{32}P-end-labeled oligonucleotide L2533 (see Fig. 5). Specific ends generated by topo I cleavage yield primer extension products that are unique to the low-density sample (lane L). Arrowheads indicate five representative examples of primer extension products for specific topo I cleavage sites. The sequence surrounding one of these sites is indicated to the right of the band that is identified with a dotted arrow. The solid arrow shows the primer extension product ending at the topo I break site in the complementary strand. Topo I (Ⓣ) is depicted attached to the 3′ end of the broken strand. Dideoxy sequencing lanes are labeled A, C, G, and T.

proteinase K step was omitted, and the samples were electrophoresed on a standard SDS-polyacrylamide protein gel and subsequently transferred to nitrocellulose. The blot was reacted with anti-human topo I antibody from scleroderma patients (45), which was shown to cross-react with the simian enzyme (A. Ching and J. Champoux, unpublished results). The results are presented in Fig. 3. Lanes 4 to 6 show the material which was isolated from cells treated in the usual way with CTT. As expected, there was no evidence of topo I in the high-density peak (lane 6). Lanes 4 and 5 show equal amounts of the low-density pool material, either treated with pancreatic DNase I (lane 4) or left untreated (lane 5). The smear of slowly migrating material in the untreated sample migrated as a series of specific bands when digested with DNase I. These bands comigrated with authentic CV-1 topo I (lane M) (molecular weight approximately 96,000) and the proteolytic breakdown products which are commonly seen in such topo I preparations. Thus, topo I was tightly associated with DNA and was present only in the low-density pool. Note that some of the sample in lane 5 was probably lost in the stacking gel owing to the low mobility of the DNA-enzyme complexes. Lanes 1 to 3 demonstrate that in the absence of CTT treatment, there was virtually no detectable topo I in either the high- or low-density fraction.

The requirement for CTT distinguishes consensus-type from non-consensus-type sites. In a series of control experiments, high- and low-density samples were prepared in the usual way, but from CV-1 cells not treated with CTT (Fig. 2A, lanes 6 and 7). As might be expected from the fact that CTT greatly enhances the amount of breakage by topo I (27), there was no evidence of specific topo I breakage in the untreated samples (Fig. 2A, compare lanes 2 and 6 at the arrowheads). This result seemed to indicate that CTT was required for protein-associated breakage of the DNA to be observed. However, an interesting exception emerged upon closer examination of the material from non-CTT-treated cells.

An example of primer extension on a low-density sample from non-CTT-treated cells is shown in Fig. 2C, lane 2. Lane 3 is the corresponding result for low-density material from CTT-treated cells. The upper arrowhead points to a non-consensus-type site (here the bands are slightly offset as a result of gel distortion), and the lower arrowhead points to a consensus-type site. The high-density samples from untreated and CTT-treated samples are shown as primer extension controls (lanes 1 and 4, respectively). The non-consensus-type site is clearly present in both the CTT-treated and untreated samples, whereas the consensus-type site is present only in the CTT-treated material. It is interesting that this non-consensus-type site is protein associated, even though it does not appear to be influenced by the presence of CTT (compare lanes 1 and 2).

To test whether CTT treatment generally distinguishes consensus-type from non-consensus-type sites, samples from CTT-treated and untreated cells were subjected to primer extension and the sequences were compared in the vicinities of 23 previously mapped break sites. Approximately half of these 23 sites had been identified as consensus-type sites, the others being non-consensus-type sites (data not shown). The consensus-type sites appeared only in the low-density samples isolated from cells treated with CTT (12 of 12) but never in samples from untreated cells. However, when non-consensus-type sites were analyzed, 9 of 11 appeared in the absence of CTT treatment and were equally strong in both CTT-treated and untreated material. Thus, detection of consensus-type sites required the presence of CTT, whereas non-consensus-type sites were detected in the absence of the drug as well as in its presence.

The control experiment in Fig. 2B is a demonstration that the samples used in the mapping analysis indeed produce a proper primer extension product. SV40 DNA that had been CsCl purified was cut with *Eco*NI and used as a template for primer extension. This was compared with the primer extension product produced by a high-density sample cut with the same enzyme. The purified SV40 (lane 1) gave an extension product that was identical to the high-density product (lane 2), indicating that there was nothing unusual about the Hirt-extracted DNA. Both of these products ended at the predicted nucleotide, a T (see arrowhead in Fig. 2B).

Most topo I break sites mapped in vivo match the consensus sequence derived in vitro. Figure 4 shows a compilation of the sequences surrounding 56 in vivo break sites mapped in this study. All of the tabulated sites were invariably detected and were mapped in two or more independent experiments. As noted previously, there appeared to be two classes of break sites, the consensus-type sites, which conformed closely to the in vitro consensus sequence, and the non-consensus-

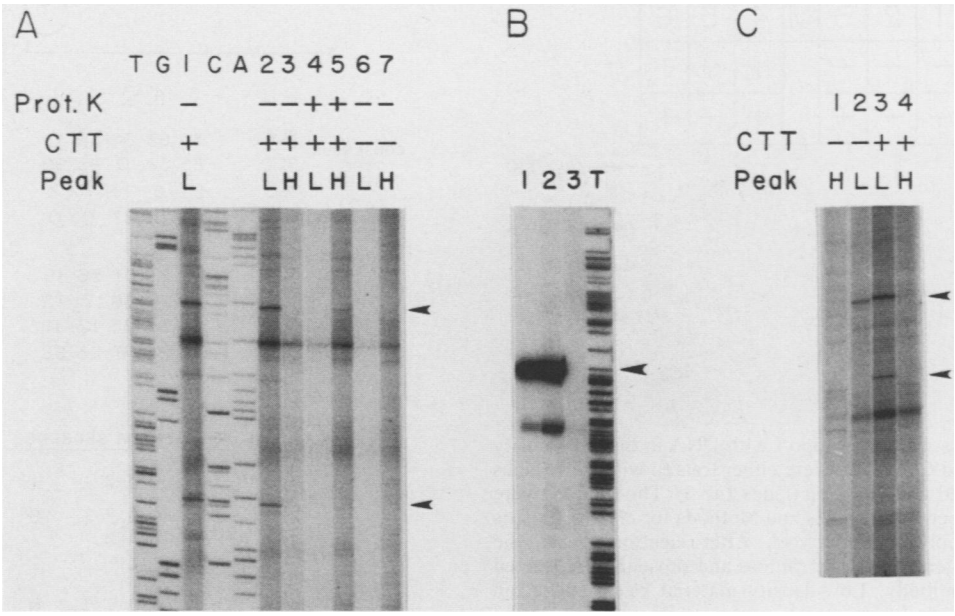

FIG. 2. CTT dependence of topo I breakage and association of protein with break sites. (A) Three sets of samples were prepared in parallel and subjected to primer extension with the ^{32}P-end-labeled oligonucleotide E4815 (see Fig. 5). One set of samples was isolated from CTT-treated CV-1 cells and prepared as described in Materials and Methods (lanes 1, 2, and 3). A second set was isolated from CTT-treated cells but treated with proteinase K before fractionation on a CsCl gradient (lanes 4 and 5). The third set of samples was prepared like the first, except that they were isolated from cells not treated with CTT (lanes 6 and 7). The dideoxy-sequencing lanes are labeled A, C, G, and T. Lanes 1, 2, 4, and 6 are primer extension products from low-density pool samples (L), and lanes 3, 5, and 7 are from high-density peak samples (H). Lanes 1 and 2 are identical and are repeated for the purpose of accurately positioning the break sites. The arrowheads mark the positions of two representative consensus-type topo I breakage sites. Less prominent sites are also visible but are not marked. (B) Control experiment showing that the high-density peak contains DNA that can serve as a template for correct primer extension upon linearization. Lane 1 contains purified SV40 DNA cut with the restriction enzyme *Eco*NI and extended to the expected nucleotide by ^{32}P-end-labeled E4815 as the primer. Lane 2 contains a sample of the high-density material, cut with *Eco*NI and extended as for lane 1. Lane 3 contains uncut high-density material primer extended from the E4815 primer. Lane T is the corresponding dideoxy T lane, for reference. The position of the correct primer extension product is indicated with an arrowhead. The lower band in lanes 1 to 3 is the product of a Klenow pause site. (C) Samples were isolated from either untreated cells (lanes 1 and 2) or CTT-treated cells (lanes 3 and 4) as described for panel A and primer extended with the end-labeled oligonucleotide E4815. The upper arrowhead marks the position of a non-consensus-type site, while the lower arrowhead indicates a consensus-type site.

type sites, which exhibited no apparent relation to the in vitro sequence. The nucleotide frequencies around the breaks are shown for the two types of sites in the top part of Fig. 4. Although the sample size was small, the non-consensus-type sites did not exhibit any obvious bias for nucleotides at specific positions, except possibly for a G at position −1. In contrast, the consensus-type sites showed preferences at the −1 through −4 positions, similar to those seen in vitro. Unlike the in vitro results, the consensus-type sites also exhibited a strong preference for G at the +1 position. Below the table is a summary of the in vivo consensus sequence derived from the 40 sites mapped. Included for comparison is a summary of the in vitro consensus, combining the information for strong and intermediate sites from that analysis (3). Possible explanations for the differences between the two consensus sequences are discussed below.

Topo I break sites are asymmetrically distributed on the SV40 genome in vivo. A summary of all the break sites mapped on the SV40 genome is shown in Fig. 5. The region labeled ori is the origin of DNA replication, including the minimal origin and auxiliary sequences that greatly enhance the efficiency of DNA replication (18). On the opposite side of the map is the region where DNA replication terminates. The terminus for the majority of replicating molecules is indicated by the hatched box (65). The early strand is in the same sense as the early mRNA, and the late strand is in the same sense as the late mRNA. The black areas indicate regions that were mapped extensively in this work (see figure legend for details). The consensus-type break sites are depicted as long arrows, and the non-consensus-type sites are shown as short lines. As discussed below, the asymmetric distribution of consensus-type sites is striking, particularly the uneven distribution of these sites along each of the strands. Also notable is the cluster of consensus-type sites in the region thought to be the major termination point for DNA replication.

The in vivo break sites mapped here clearly represent only a subset of the potential topo I break sites. In the regions mapped, there are a total of 487 sites that match the in vitro consensus sequence (data not shown). However, not all sites that match the consensus sequence are actually broken by topo I in vitro. On the basis of the in vitro breakage frequencies (3), we estimate that topo I would break approximately 77% of the sites that match the consensus sequence. Thus, of the 487 sites present in the regions mapped, only 375 (77%) would have been observed as break sites in vitro. Only these 375 sites can be considered potential in vivo break sites, and of these 375 potential break sites, only 40 were actually observed as break sites in vivo. In both the ori and termination regions there were as many potential topo I sites on the late strand as on the early strand, yet within any one region, most of the break sites observed were restricted

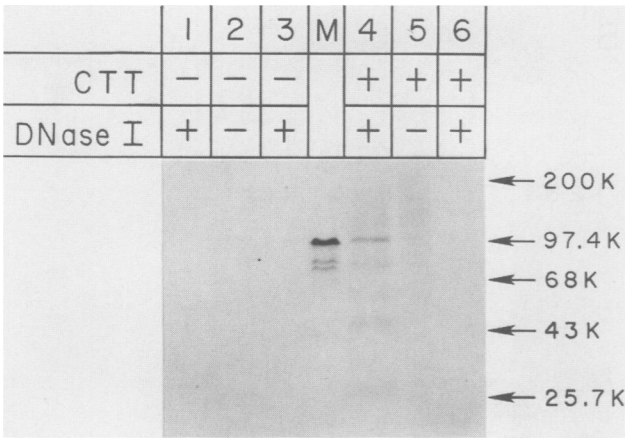

FIG. 3. Tight association of topo I with DNA in the low-density peak. SV40-infected CV-1 cells were either treated with CTT (lanes 4 to 6) or not treated with the drug (lanes 1 to 3). The samples were prepared as described in Materials and Methods for electrophoresis through an SDS-polyacrylamide gel. After electrophoresis, the samples were transferred to nitrocellulose and subsequently reacted with anti-topo I antibody. Low-density material was analyzed in lanes 2 through 5. Samples in lanes 3 and 4 were treated with DNase I prior to electrophoresis, while the material in lanes 2 and 5 was left untreated. The high-density peak samples were treated with DNase I (lanes 1 and 6) to consolidate any potential topo I band that might be present. Lane M contains a CV-1 whole-cell extract run as a marker for topo I.

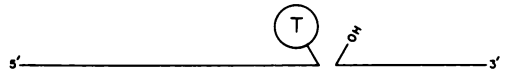

		-5	-4	-3	-2	-1	+1	+2	+3
CONSENSUS TYPE SITES (40)	%A	30	63	30	55	0	15	55	30
	%T	25	32	0	45	98	3	23	20
	%C	25	5	13	0	2	2	12	15
	%G	20	0	57	0	0	80	10	35
NON-CONSENSUS TYPE SITES (16)	%A	25	13	31	56	19	19	56	25
	%T	31	25	38	7	13	19	13	38
	%C	6	37	25	12	0	12	0	0
	%G	38	25	6	25	68	50	31	37

CONSENSUS SEQUENCE SUMMARY

	-4	-3	-2	-1	+1
IN VIVO	A	G	T	T	G
	T	A	A		
			(C)		
IN VITRO	A	G	T	T	N
	T	C	A	(C)	
				(A)	

FIG. 4. Compilation of nucleotides surrounding in vivo topo I break sites. The upper diagram represents a topo I breakage product containing a free 5′ hydroxyl and the enzyme covalently bound to the 3′ end of the DNA. The percent occurrences for the four nucleotides at eight positions across the break site are shown in tabular form below the diagram. The upper table includes the 40 consensus-type sites mapped in this work. The lower table shows the results for the 16 sites which did not conform to the known in vitro consensus. Below the numerical tables is a summary of the consensus sequence for the in vivo topo I breakage sites analyzed here. The in vitro consensus (3) is included for comparison. Following is a list of all sites detected in this analysis (66 sites), including those sites for which the break point was not precisely defined. The number refers to the −1 position of the break site, the nucleotide to which the enzyme becomes covalently attached. The break site is on the strand that is the same sense as the late mRNA if the number has an L prefix; it is on the strand that is the same sense as the early mRNA if the number has an E prefix. Sites in quotation marks have not been mapped precisely. Sites: L2299, L2265, L2257, L2245, L2194, L2073, L2325, L2059, L"2184-7", E2606, E2635, E2664, E2669, E2657, E2672, E2673, E2688, E2735, E"2869-70", E2880, E2910, E2913, E2874, E"3029-30", E2384, E2487, E2529, E2303, E2416, E2355, E2321, E2578, E2401, L2808, L2758, L2753, L2733, L2615, L2502, L2495, L2668, L"5113-6", L5059, L4955, L4889, E4888, E4930, E4972, E5000, E5020, E5047, E5075, E"5101-3", E5209, E"62-7", E"178-9", E"410-11", L"384-5", L370, L335, L309, L"226-7", L199, L194, L127, and L122.

to only one of these strands. Another unusual feature of the break site distribution is that there were more consensus-type break sites detected in the termination region than in the ori region. Overall, there were 2.5 times more sites broken per unit length of DNA in the termination region, even though this area has only 1.4 times as many potential break sites as the ori region.

DISCUSSION

In vivo topo I break sites were mapped on SV40 DNA by using the drug CTT to increase the amount of breakage to a detectable level. This is the first time the primer extension technique has been used to map topo I break sites, allowing a large number of sites to be mapped to the nucleotide level. Any interpretation of these mapping data depends on a knowledge of the effects of CTT on the specificity of topo I breakage. Champoux and Aronoff (in press) have found that the drug has little effect on the breakage pattern of the wheat germ enzyme in vitro, although breakage at some sites is enhanced more than breakage at others. Similar results have been reported by Kjeldsen et al. (32) for the human topo I. On the basis of these studies, we assume that the drug has little or no effect on the breakage specificity of topo I in vivo. However, we have not attempted to categorize the strength of the in vivo break sites, since CTT does enhance the in vitro breakage of some sites preferentially. In mapping topo I sites near *Tetrahymena* rDNA, a very strong break site was found within a repeated hexadecameric sequence (1, 4). This sequence was also a preferred break site for mammalian topo I in vitro. In the present study, no site mapped was significantly stronger than any other site. However, since the hexadecameric sequence is not present in SV40 DNA, it is difficult to correlate these results.

Although most of the in vivo break sites match the consensus sequence previously determined in vitro (see below), some of the sites do not show any similarity to the in vitro consensus sequence. As a class, the non-consensus-type sites do not have any common sequence features except perhaps a bias toward G residues at the −1 position. Another difference between these sites and the consensus-type sites is that although they are protein associated, the non-consensus-type sites are broken with equal efficiency in the absence as well as the presence of CTT. Note that even though these sites are protein associated, the protein need not necessarily be located at the site of the break.

The origin of the non-consensus-type break sites remains unclear. They could be the result of topo II action, although the sequences surrounding these sites do not conform to the topo II consensus sequence (50) with any frequency greater

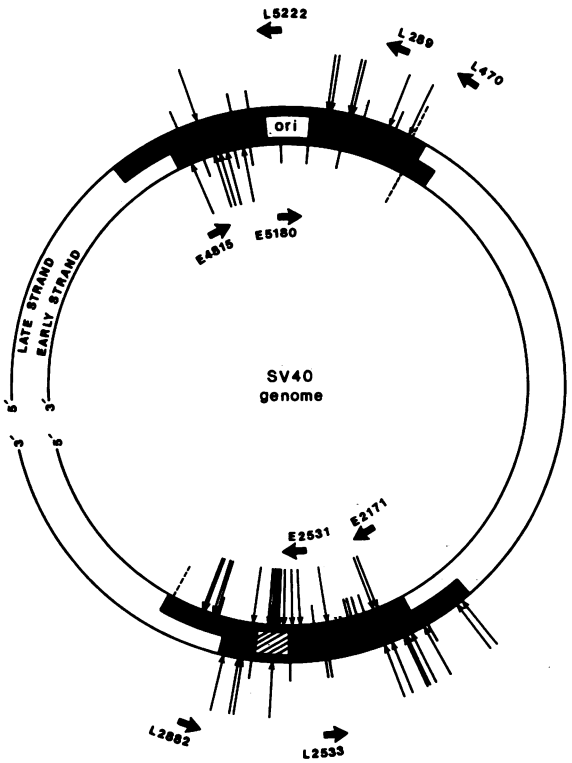

FIG. 5. Distribution of in vivo topo I break sites on SV40 DNA. The circle represents the SV40 genome. The strand marked LATE is in the same sense as the late mRNA; the strand marked EARLY is in the same sense as the early mRNA. The numbering system is that of Buchman et al. (7). The ori region encompasses the minimal origin of DNA replication, as well as the flanking auxiliary sequences (5, 18). Symbols: ▨, range for termination of replication in wild-type SV40 molecules (65); ▬, sections of the two strands mapped in this work. The actual nucleotide limits of the mapped areas are as follows: ori region late strand, nucleotides 445 to 4745, ori region early strand, nucleotides 4844 to 500; termination region early strand, nucleotides 2197 to 3020; termination region late strand, nucleotides 2816 to 2025. Consensus-type sites (→) and non-consensus-type sites (—) are shown, as are sites that have not been mapped to the nucleotide (- - - -). The oligonucleotides used as primers in the primer extension reactions are shown as thick arrows above or below the strand to which they are complementary. The oligonucleotides with an E prefix are complementary to the early strand and thus are the same sense as the late strand. The reverse is true for oligonucleotides with an L prefix. The number represents the nucleotide number of the SV40 genome that matches the 5′ end of the oligonucleotide; e.g., oligonucleotide E4815 matches the sense of the late strand and spans nucleotides 4815 to 4832 on the SV40 map.

than would occur by chance. Also, topo II breakage of DNA has not been observed except in the presence of specific inhibitors (50). It is possible that the non-consensus-type sites are the result of primer extension to the ends of DNA strands that are still being synthesized, such as Okazaki fragments. Some of the non-consensus-type sites are in the vicinity of the 5′ ends of nascent DNA chains, as mapped by Hay and DePamphilis (24). One non-consensus-type site (E5209) mapped 2 bases from a start site for continuous-strand synthesis at the ori (24). The non-consensus-type sites could be break sites of a yet-to-be discovered topoisomerase that is not affected by CTT. Since the sites are protein associated, they could conceivably be the result of a protein-priming mechanism for SV40 DNA replication similar to the priming mechanism of the adenovirus terminal protein (9, 35).

The majority of the break sites mapped in this analysis conform to the consensus sequence: 5′-A/T-G/A/(C)-T/A-T-BREAK-G-3′. This is very similar to the consensus sequence determined in vitro for strong rat topo I break sites (3). There are, however, notable differences. The in vivo sites exhibit a distinct preference for a G after the break (the +1 position) and a stronger bias for T as the nucleotide to which topo I becomes attached. Also, the preference for A at the −3 position is slightly greater for the in vivo sites than for the in vitro sites. These differences could have several possible origins. For instance, the simian enzyme characterized here might have a slightly different sequence specificity from that of the rat enzyme used in the in vitro study. The differences could also be due to the presence of the drug CTT in one case but not the other, although, as mentioned above, the presence of CTT does not have a significant effect on the in vitro consensus sequence of wheat germ topo I (Champoux and Aronoff, in press). Alternatively, the in vivo consensus sequence for breakage might be a reflection of the chromatinized state of the DNA in vivo or the result of some other structural feature not present in vitro.

Several investigators have noted that the sequences surrounding the crossover sites for illegitimate recombination frequently contain the in vitro consensus sequence for topo I breakage (8, 15, 26, 29, 66, 67). Combining this observation with the fact that topo I can join two DNA strands under special circumstances in vitro, an in vivo role for the enzyme in illegitimate recombination has been proposed (8, 15). This proposal was based on the assumption that the consensus sequence recognized by the enzyme in vivo is the same as the consensus sequence determined in vitro. The data presented here show that this assumption is valid.

The distinction between the topo I break sites mapped here and potential topo I break sites is important. Of the 375 potential break sites present in the regions mapped, only 40 (11%) were actually broken by topo I in vivo. Some sections of the SV40 genome examined in this study were the same as those used in the in vitro analysis (3), yet many of the sites broken in vitro were not found to be topo I break sites in vivo. It is possible that some topo I break sites were below the threshold of detection in this analysis and were thus not identified. Another possible reason for the observed difference is that in vivo, topo I has limited access to the DNA. Perhaps potential break sites are masked by DNA-binding proteins such as histones. Alternatively, topo I could be attracted to certain sites by specific interactions involving protein-protein contacts.

Since a number of studies have shown topo I to be associated with transcriptionally active genes, it is possible that the break site distribution seen here is related to viral gene transcription as opposed to DNA replication. Although we cannot rigorously exclude this possibility, it seems unlikely for a number of reasons. First, the transcribing molecules represent only 1% of the total SV40 molecules late in infection (37). We found that 7 to 10% of the total SV40 DNA had shifted to the low-density position after CTT treatment. Thus, less than 15% of the low-density DNA could be transcription complexes. Second, it has been demonstrated that after CTT treatment in vivo, topo I is preferentially associated with replicating molecules and that the low-density peak is enriched for these replicating molecules (14). Third, it has been shown that late in infection there is 20 times more transcription of late genes than of early genes (34). If the consensus-type sites mapped here were a reflec-

tion of topo I involvement in transcription, we might expect to find 20 times more consensus-type sites in the late region of the SV40 genome than in the early region. The absence of this type of asymmetry is consistent with the idea that the low-density material has a small proportion of transcribing molecules.

The in vivo topo I break sites mapped in this study did not have an obvious nucleosomelike pattern with a 200-base-pair repeat. This is not surprising, since a regular, repeated pattern of nucleosomes would not be evident unless the nucleosomes were very tightly phased, apparently an extremely rare occurrence in native chromatin (for reviews, see references 20 and 30). In one study, a nucleosomelike pattern of topo I break sites was observed for actively transcribed chromatin in *Xenopus* oocytes (17). The fact that the SV40 sites mapped here are most probably associated with replicating rather than transcribing DNA could account for the differences between the two studies.

Although the topo I break sites do not appear to exhibit a pattern related to the nucleosomal repeat, the distribution of break sites is not random. The pattern of site distribution is asymmetrical on the areas of SV40 mapped, and there are three ways that this asymmetry is manifested. First, there is a regional asymmetry in that 2.5 times more sites are broken near the terminus of DNA replication than at the ori. This is not due purely to a difference in the number of potential break sites, as discussed above. Second, within the ori region there is a striking asymmetry to the early- versus late-strand distribution of topo I break sites, centered around the start of bidirectional replication (24). The consensus-type sites are found almost exclusively on the strand that is the template for discontinuous DNA synthesis. The same pattern is seen approximately 180° away, near the terminus of DNA replication, although the asymmetry is not as strong as near the ori. A third type of asymmetry is revealed as a prominent strand-specific cluster of topo I sites within the region that is the preferred site for replication termination (54, 65).

Assuming that the topo I sites mapped here are indeed associated with replicating SV40 DNA, the site distribution should reflect the interaction of topo I molecules with the entire pool of replicating SV40 molecules in the infected cell. Thus, the site distribution probably represents the prevalence of particular replicative intermedites in the pool, rather than the prevalence of topo I at a particular site on every molecule. It is interesting that SV40 replication is known to pause near the end of replication and replicative intermediates that are close to completion are found to accumulate (56). This might explain the prevalence of topo I break sites near the terminus. Also consistent with this clustering at the terminus is the possibility that topo I is involved in the separation of daughter molecules during the termination of replication. There are two models for the termination of SV40 DNA replication. One model suggests that termination occurs via a catenated dimer intermediate (53). The other model suggests that the two daughter molecules are separated before DNA synthesis is complete, resulting in uncoupled replicative intermediates that have gaps near the terminus (55, 65). This separation could take place through the nicking-closing action of topo I; thus, a cluster of topo I sites might be expected near the region of termination.

If topo I provides the swivels to relieve superhelical tension generated during DNA replication, two extreme hypotheses could be envisioned for the topological organization of the enzyme on replicative intermediates. The first is that topo I acts as a localized intermittent swivel for all stages of replication at only one position on the SV40 genome, and this position is where replication usually terminates, 180° away from the origin. The other hypothesis is that topo I action is tightly coordinated with the movement of the replication fork and that the enzyme acts just in front of the advancing fork. Assuming that the sites mapped here reflect the distribution of topo I on the population of replicating SV40 molecules, the first hypothesis is ruled out by the data, since topo I sites were found in both the terminus and ori regions. Note that an intermediate model in which topo I acts randomly ahead of the replication fork is also consistent with the data.

The strand asymmetry of topo I distribution might be explained by supposing that the enzyme is associated with the replication complex. Recent evidence showing an association between topo I and SV40 replication forks is consistent with this suggestion (2). DNA replication is inherently asymmetrical, since DNA polymerases synthesize only in the 5′-to-3′ direction. If topo I was coordinated spatially with the replication machinery, its distribution on the template would also be asymmetrical. Thus, instead of relieving the superhelical tension by acting at sites far removed from the replication fork, topo I could be positioned near the fork, continually relieving the tension generated by the moving replication machinery. Although this positioning does not explain the preferential association of topo I with the strand that is the template for discontinuous synthesis, it could explain the asymmetric distribution of topo I, and it also suggests that topo I action during DNA replication is not random but is coordinated with the entire replication process.

ACKNOWLEDGMENTS

We thank Alison Rattray and Andrew Ching for helpful comments during the preparation of the manuscript.

This work was supported by grant DMB-8603208 from the National Science Foundation.

LITERATURE CITED

1. **Anderson, A. H., E. Gocke, B. J. Bonven, O. F. Nielsen, and O. Westergaard.** 1985. Topoisomerase I has a strong binding preference for a conserved hexadecameric sequence in the promoter region of the rRNA gene from *Tetrahymena pyriformis*. Nucleic Acids Res. **13**:1543–1557.
2. **Aveman, K., R. Knippers, T. Koller, and J. M. Sogo.** 1988. Camptothecin, a specific inhibitor of type I DNA topoisomerase, induces DNA breakage at replication forks. Mol. Cell. Biol. **8**:3026–3034.
3. **Been, M. D., R. R. Burgess, and J. J. Champoux.** 1984. Nucleotide sequence preference at rat liver and wheat germ type 1 DNA topoisomerase breakage sites in duplex SV40 DNA. Nucleic Acids Res. **12**:3097–3114.
4. **Bonven, B. J., E. Gocke, and O. Westergaard.** 1985. A high affinity topoisomerase I binding sequence is clustered at DNase I hypersensitive sites in Tetrahymena r-chromatin. Cell **41**: 541–551.
5. **Brady, J., C. E. Buckler, and N. Salzman.** 1987. Simian virus 40 genetic map, p. 64–69. *In* S. J. O'Brian (ed.), Genetic maps 1987. Cold Spring Harbor Laboratory, Cold Spring Harbor, N.Y.
6. **Brill, S. J., S. DiNardo, K. Voelkel-Meiman, and R. Sternglanz.** 1987. Need for DNA topoisomerase I activity as a swivel for DNA replication and for transcription of ribosomal RNA. Nature (London) **326**:414–416.
7. **Buchman, A. R., L. Burnett, and P. Berg.** 1981. The SV40 nucleotide sequence, p. 799–823. *In* J. Tooze (ed.), DNA tumor viruses, 2nd ed. Cold Spring Harbor Laboratory, Cold Spring Harbor, N.Y.
8. **Bullock, P., J. J. Champoux, and M. Botchan.** 1985. Association

of crossover points with topoisomerase I cleavage sites: a model for nonhomologous recombination. Science **230**:954–958.
9. **Challberg, M. D., S. V. Desiderio, and T. J. Kelly, Jr.** 1980. Adenovirus DNA replication in vitro: characterization of a protein covalently linked to nascent DNA strands. Proc. Natl. Acad. Sci. USA **77**:5105–5109.
10. **Champoux, J. J.** 1976. Evidence for an intermediate with a single-strand break in the reaction catalyzed by the DNA untwisting enzyme. Proc. Natl. Acad. Sci. USA **73**:3488–3491.
11. **Champoux, J. J.** 1977. Strand breakage by the DNA untwisting enzyme results in the covalent attachment of the enzyme to DNA. Proc. Natl. Acad. Sci. **74**:3800–3804.
12. **Champoux, J. J.** 1978. Mechanism of the reaction catalyzed by the DNA untwisting enzyme: attachment of the enzyme to the 3′-terminus of the nicked DNA. J. Mol. Biol. **118**:441–446.
13. **Champoux, J. J.** 1981. DNA is linked to the rat liver DNA nicking-closing enzyme by a phosphodiester bond to tyrosine. J. Biol. Chem. **256**:4805–4809.
14. **Champoux, J. J.** 1988. Topoisomerase I is preferentially associated with isolated replicating simian virus 40 molecules after treatment of infected cells with camptothecin. J. Virol. **62**: 3675–3683.
15. **Champoux, J. J., and P. A. Bullock.** 1988. A possible role for the eucaryotic type I topoisomerase in illegitimate recombination, p. 655–666. *In* R. Kucherlapati and G. Smith (ed.), Genetic recombination. American Society for Microbiology, Washington, D.C.
16. **Champoux, J. J., W. K. McCoubrey, and M. D. Been.** 1984. DNA structural features that lead to strand breakage by eukaryotic type-I topoisomerase. Cold Spring Harbor Symp. Quant. Biol. **49**:435–442.
17. **Culotta, V., and B. Sollner-Webb.** 1988. Sites of topoisomerase I action on X. laevis ribosomal chromatin: transcriptionally active rDNA has an approx. 200 bp repeating structure. Cell **52**:585–597.
18. **DePamphilis, M. L., R. S. Decker, M. Yamaguchi, R. Possenti, D. O. Wirak, R. Perona, and J. A. Hassell.** 1987. Transcriptional elements and their role in activation of simian virus 40 and polyoma virus origins of replication. UCLA Symp. Mol. Cell. Biol. **47**:367–379.
19. **DiNardo, S., K. A. Voelkel, and R. Sternglanz.** 1982. Escherichia coli DNA topoisomerase I mutants have compensatory mutations in DNA gyrase genes. Cell **31**:43–51.
20. **Eissenberg, J. C., I. L. Cartwright, G. H. Thomas, and S. C. R. Elgin.** 1985. Selected topics in chromatin structure. Annu. Rev. Genet. **19**:485–536.
21. **Gilmour, D. S., and S. C. R. Elgin.** 1987. Localization of specific topoisomerase I interactions within the transcribed region of active heat shock genes by using the inhibitor camptothecin. Mol. Cell. Biol. **7**:141–148.
22. **Gilmour, D. S., G. Pflugfelder, J. C. Wang, and J. T. Lis.** 1986. Topoisomerse I interacts with transcribed regions in Drosophila cells. Cell **44**:401–407.
23. **Halligan, B. D., J. L. Davis, K. A. Edwards, and L. F. Liu.** 1982. Intra- and intermolecular strand transfer by HeLa DNA topoisomerase I. J. Biol. Chem. **257**:3995–4000.
24. **Hay, R. T., and M. L. DePamphilis.** 1982. Initiation of SV40 DNA replication in vivo: location and structure of 5′ ends of DNA synthesized in the ori region. Cell **28**:767–779.
25. **Hirt, B.** 1967. Selective extraction of polyoma DNA from infected mouse cell cultures. J. Mol. Biol. **26**:365–369.
26. **Hogan, A., and E. A. Faust.** 1986. Nonhomologous recombination in the parvovirus chromosome: role for a CTA/TTTC/T motif. Mol. Cell. Biol. **6**:3005–3009.
27. **Hsiang, Y.-H., R. Hertzberg, S. Hecht, and L. F. Liu.** 1985. Camptothecin induces protein-linked DNA breaks via mammalian DNA topoisomerase I. J. Biol. Chem. **260**:14873–14878.
28. **Hsieh, C.-H., and J. D. Griffith.** 1988. The terminus of SV40 DNA replication and transcription contains a sharp sequence-directed curve. Cell **52**:535–544.
29. **Hyrien, O., M. Debatisse, G. Buttin, and B. R. De Saint Vincent.** 1987. A hotspot for novel amplification joints in a mosaic of Alu-like repeats and palindromic A + T-rich DNA. EMBO J. **6**:2401–2408.
30. **Igo-Kemenes, T., W. Hoerz, and H. G. Zachau.** 1982. Chromatin. Annu. Rev. Biochem. **51**:89–121.
31. **Jakobovits, E. B., S. Bratosin, and Y. Aloni.** 1980. A nucleosome-free region in SV40 minichromosomes. Nature (London) **285**:263–265.
32. **Kjeldsen, E., S. Mollerup, B. Thomsen, B. J. Bonven, L. Bolund, and O. Westergaard.** 1988. Sequence-dependent effect of camptothecin on human topoisomerase I DNA cleavage. J. Mol. Biol. **202**:333–342.
33. **Laemmli, U. K.** 1970. Cleavage of structural proteins during the assembly of the head of bacteriophage T4. Nature (London) **227**:680–685.
34. **Laub, O., and Y. Aloni.** 1975. Transcription of simian virus 40. V. Regulation of simian virus 40 gene expression. J. Virol. **16**:1171–1183.
35. **Lichy, J. H., M. S. Horowitz, and J. Hurwitz.** 1981. Formation of a covalent complex between the 80,000-dalton adenovirus terminal protein and 5′-dCMP in vitro. Proc. Natl. Acad. Sci. USA **78**:2678–2682.
36. **Liu, L. F., and J. C. Wang.** 1987. Supercoiling of the DNA template during transcription. Proc. Natl. Acad. Sci. USA **84**:7024–7027.
37. **Llopis, R., F. Perrin, F. Bellard, and P. Gariglio.** 1981. Quantitation of transcribing native simian virus 40 minichromosomes extracted from CV-1 cells late in infection. J. Virol. **38**:82–90.
38. **Maniatis, T., E. F. Fritsch, and J. Sambrook.** 1982. Molecular cloning: a laboratory manual. Cold Spring Harbor Laboratory, Cold Spring Harbor, N.Y.
39. **Maxwell, A., and M. Gellert.** 1986. Mechanistic aspects of DNA topoisomerases. Adv. Protein Chem. **38**:69–107.
40. **McCoubrey, W. K., and J. J. Champoux.** 1986. The role of single-strand breaks in the catenation reaction catalyzed by the rat type I topoisomerase. J. Biol. Chem. **261**:5130–5137.
41. **Mengeritsky, G., and E. N. Trifonov.** 1984. Nucleotide sequence-directed mapping of the nucleosomes of SV40 chromatin. Cell Biophys. **6**:1–8.
42. **Milavetz, B.** 1986. Analysis of the origin-specific nucleosome-free region in SV40 encapsidation intermediates. Virology **153**: 310–313.
43. **Pruss, G. J., S. H. Manes, and K. Drlica.** 1982. Escherichia coli DNA topoisomerase I mutants: increased supercoiling is corrected by mutations near gyrase genes. Cell **31**:35–42.
44. **Saragosti, S., S. Cereghini, and M. Yaniv.** 1982. Fine structure of the regulatory region of simian virus 40 minichromosomes revealed by DNase I digestion. J. Mol. Biol. **160**:133–146.
45. **Shero, J. H., B. Bordwell, N. F. Rothfield, and W. C. Earnshaw.** 1986. High titers of autoantibodies to topoisomerase I (Scl-70) in sera from scleroderma patients. Science **231**:737–740.
46. **Snapka, R. M.** 1986. Topoisomerase inhibitors can selectively interfere with different stages of simian virus 40 DNA replication. Mol. Cell. Biol. **6**:4221–4227.
47. **Snapka, R. M., M. A. Powelson, and J. M. Strayer.** 1988. Swiveling and decatenation of replicating simian virus 40 genomes in vivo. Mol. Cell. Biol. **8**:515–521.
48. **Sogo, J. M., H. Stahl, T. Koller, and R. Knippers.** 1986. Structure of replicating simian virus 40 minichromosomes. J. Mol. Biol. **189**:189–204.
49. **Solomon, M. J., and A. Varshavsky.** 1987. A nuclease-hypersensitive region forms de novo after chromosome replication. Mol. Cell. Biol. **7**:3822–3825.
50. **Spitzner, J. R., and M. T. Muller.** 1988. A consensus sequence for cleavage by vertebrate DNA topoisomerase II. Nucleic Acids Res. **16**:5533–5556.
51. **Stewart, A. F., and G. Schutz.** 1987. Camptothecin-induced in vivo topoisomerase I cleavages in the transcriptionally active tyrosine aminotransferase gene. Cell **50**:1109–1117.
52. **Stillman, B.** 1986. Chromatin assembly during SV40 replication in vitro. Cell **45**:555–565.
53. **Sundin, O., and A. Varshavsky.** 1981. Arrest of segregation leads to accumulation of highly intertwined catenated dimers: dissection of the final stages of SV40 DNA replication. Cell **25**:659–669.

54. **Tack, L. C., and G. N. Proctor.** 1987. Two major replicating simian virus 40 chromosome classes. Synchronous replication fork movement is associated with bound large T antigen during elongation. J. Biol. Chem. **262**:6339–6349.
55. **Tapper, D. P., S. Anderson, and M. L. DePamphilis.** 1982. Distribution of replicating simian virus 40 DNA in intact cells and its maturation in isolated nuclei. J. Virol. **41**:877–892.
56. **Tapper, D. P., and M. L. DePamphilis.** 1978. Discontinuous DNA replication: accumulation of simian virus 40 DNA at specific stages in its replication. J. Mol. Biol. **120**:401–422.
57. **Tegtmeyer, P., C. Dohan, and C. Reznikoff.** 1970. Inactivating and mutagenic effects of nitrosoguanidine on simian virus 40. Proc. Natl. Acad. Sci. USA **66**:745–752.
58. **Thrash, C., K. Voelkel, S. DiNardo, and R. Sternglanz.** 1984. Identification of Saccharomyces cerevisiae mutants deficient in DNA topoisomerase I activity. J. Biol. Chem. **259**:1375–1377.
59. **Tooze, J. (ed.).** 1981. DNA tumor viruses, 2nd ed. Cold Spring Harbor Laboratory, Cold Spring Harbor, N.Y.
60. **Varshavsky, A. J., O. Sundin, and M. Bohn.** 1979. A stretch of "late" SV40 viral DNA about 400 bp long which includes the origin of replication is specifically exposed in SV40 minichromosomes. Cell **16**:453–466.
61. **Vishwanatha, J. K., M. Yamaguchi, M. L. DePamphilis, and E. F. Baril.** 1986. Selection of template initiation sites and the lengths of RNA primers synthesized by DNA primase are strongly affected by its organization in a multiprotein DNA polymerase alpha complex. Nucleic Acids Res. **14**:7305–7323.
62. **Vosberg, H.-P.** 1985. DNA topoisomerases: enzymes that control DNA conformation. Curr. Top. Microbiol. Immunol. **114**: 19–102.
63. **Wang, J. C.** 1985. DNA topoisomerases. Annu. Rev. Biochem. **54**:665–697.
64. **Wang, J. C.** 1987. Recent studies of DNA topoisomerases. Biochim. Biophys. Acta **909**:1–9.
65. **Weaver, D. T., S. C. Fields-Berry, and M. L. DePamphilis.** 1985. The termination region for SV40 DNA replication directs the mode of separation for the two sibling molecules. Cell **41**: 565–575.
66. **Wilkie, T. M., and R. D. Palmiter.** 1987. Analysis of the integrant in MyK-103 transgenic mice in which males fail to transmit the integrant. Mol. Cell. Biol. **7**:1646–1655.
67. **Williams, T. J., and M. Fried.** 1986. Inverted duplication-transposition event in mammalian cells at an illegitimate recombination join. Mol. Cell. Biol. **6**:2179–2184.
68. **Wu, H.-Y., S. Shyy, J. C. Wang, and L. F. Liu.** 1988. Transcription generates positively and negatively supercoiled domains in the template. Cell **53**:433–440.
69. **Yang, L., and L. F. Liu.** 1987. The roles of DNA topoisomerases in SV40 DNA replication. UCLA Symp. Mol. Cell. Biol. **47**:315–326.
70. **Yang, L., M. S. Wold, J. J. Li, T. J. Kelly, and L. F. Liu.** 1987. Roles of DNA topoisomerases in simian virus 40 DNA replication in vitro. Proc. Natl. Acad. Sci. USA **84**:950–954.
71. **Zhang, H., J. C. Wang, and L. F. Liu.** 1988. Involvement of DNA topoisomerase I in the transcription of human ribosomal RNA genes. Cell **85**:1060–1064.